Theoretical and experimental investigation on the linear growth rate of the thermo-acoustic combustion instability

Theoretical and experimental investigation on the linear growth rate of the thermo-acoustic combustion instability

M. Kojourimanesh[*, 1], V. Kornilov[1], I. Lopez Arteaga[1, 2], L.P.H. de Goey[1]

[1]Dept. of Mechanical Engineering, Eindhoven University of Technology, The Netherlands
[2]Dept. of Engineering Mechanics, KTH Royal Institute of Technology, Sweden

Abstract

A systematic measurement of the linear growth rate and frequency of the oscillation at the onset of thermo-acoustic combustion instability is reported and compared with the results of theoretical approaches. To do so, a specialized setup with a passive control device has been developed. The setup allows quick switching between the stable and unstable operation of the system by switching the upstream boundary condition of the burner/flame from the almost anechoic termination to the closed end. The measurements have been done for a burner with premixed burner-stabilized Bunsen-type flames. When the rate of growth is slow, which means that the time of the linear growth of the oscillation is larger than the switching time, (about 0.01 seconds), the growth rate and the instability onset frequency can be measured accurately. This paper endeavors to make a comparison between the theoretical results of modeling strategies and experimental findings. Two modeling strategies are tested. Within the first approach, one has to measure the frequency response of the combustion appliance from two sides at the one cross-section area, 1) the burner including the flame and downstream sides of the burner/flame as an acoustically active element; 2) reflection coefficient of the upstream side of the burner/flame. Then by applying a system identification procedure, (thermo)-acoustic responses in the complex domain can be obtained. Finally, complex eigen frequency can be calculated by solving the corresponding dispersion equation. The alternative approach was proposed by Kopitz and Polifke in 2008 and allows estimating both the frequency of oscillation and the growth rate from a polar plot of the system's characteristic equation in the frequency domain. Both methods are tested and compared with experimental findings. The comparison between experimental and modeling results shows that the unstable frequencies can be predicted accurately by both tested modeling strategies. The prediction of the instabilities growth rates is closer to the measured one when the modeling in the Complex (Laplace) domain is used. However, the frequency domain analysis provides less accurate, but still reasonable estimates of the growth rates.

Introduction

Thermoacoustic instability has been a serious impediment to the design of burners or combustor systems. Although great progress has been made in the thermoacoustic design of combustion systems such as jet engines, gas turbines, and boilers in recent years, companies still face this kind of instability in their products. Determining and understanding roots of instability are challenging, so simplifying the system analysis based on network modeling [1], preparing a lab-scaled sample of burners [2], finding Flame Transfer Function (FTF) [3] or Flame Describing Function (FDF) [4], and making acoustical models of the upstream and downstream of the flame/burner [5] are considered as methodologies to study the phenomenon.

The typical practically relevant output of the models is the prediction of the system complex eigen frequencies. Experimentally, measuring of the unstable frequency is an easy task that can be done by a microphone. however, measuring the growth/decay rate is challenging. In the thermoacoustic field, only few attempts are described for measuring the growth/decay rate experimentally and comparing them with theoretical models [6–11].

The goal of this paper is to propose a new method to measure complex frequencies experimentally and make a comparison with theoretical results of two modeling strategies. The first strategy is based on the complex domain (Laplace domain). A frequent practice is to measure FTF and acoustic Reflection Coefficient (RC) of the upstream and downstream sides of the burner/flame, called R_{up} and R_{dn}, then create the system matrix with the help of network modeling. Next, one has to search for the roots of the matrix's determinant in the complex plane, s, to get a set of eigenfrequencies of the thermoacoustic system. However, Kojourimanesh et al. [12] have shown that instead of measuring the FTF and the RC at the hot side of the flame, it would be much easier to measure RC of a combination of the FTF with the downstream side, called R_{in}, at a cross-section area in the cold side. R_{up} should also be measured at that cross-section area. Then, roots of $1\text{-}R_{in}(s)\,R_{up}(s)$ in the complex domain provide the same eigenfrequencies of the system.

On the other hand, for the second strategy, only the frequency domain analysis is applied. In 2008, Kopitz and Polifke [13] proved that the unstable frequency and the growth/decay rate can be calculated from the polar plot of the Open-Loop system Transfer Function (OLTF). To determine the OLTF of the thermo-acoustic system, Computational Fluid Dynamics (CFD) and low-order network modeling were combined. They showed that the unstable frequency is approximately equal to the frequency where the distance between the polar plot of OLTF and the critical point (-1) attains a local minimum.

[*] Corresponding author: m.kojourimanesh@tue.nl

The growth/decay rate is approximately equal to the minimum distance from the critical point to the OLTF image curve divided by the scaling factor of the mapping [13]. However, it would be also easier to measure R_{in} and R_{up} instead of finding OLTF or measuring the FTF and R_{dn}. Then, the assessment of the polar plot of the measured $1\text{-}R_{in}(f)\,R_{up}(f)$ function in the frequency domain would serve for determining the (in)stability. If the graph turns around the origin, then the system will be unstable, otherwise it will be stable for the case of a causal function.

In this work, these two strategies are evaluated with the experimental data for various conditions of the upstream and downstream sides. A damper including a ball valve has been used at the upstream side to provide a closed-end and semi-anechoic end. To make different acoustic conditions at the downstream side, ten innovative terminations have been used. The terminations have the magnitude of reflection coefficients from 0.1 to 1 almost independent from the frequency.

Formulation

Network modeling, used in this study, describes the relationship between the RC of upstream, R_{up}, and downstream, R_{dn}, sides of the flame/burner in a thermo-acoustic system. By considering linear acoustical plane waves with zero mean flow Mach number; the relations between Riemann invariants at both sides of the flame with Flame Transfer Matrix (FTM), produce a homogeneous system of linear equations [12,14]. A nontrivial solution of the system is derived when the determinant of the system matrix would be zero. A corresponding dispersion relation for this kind of network modeling is widely used in recent studies, see for instance [12,14–16]. It can be written as

$$\mathbf{1} - \boldsymbol{R_{up}(s)\,R_{in}(s)} = \mathbf{0}. \quad (1)$$

In this equation, R_{in} is the input reflection coefficient of the burner/flame terminated by R_{dn} shown in Fig. 1. The acoustic properties of the flame/burner and downstream part of an appliance are incorporated in R_{in}. The crucial advantage of this representation is that it requires only two separate acoustical measurements of R_{in} and R_{up}.

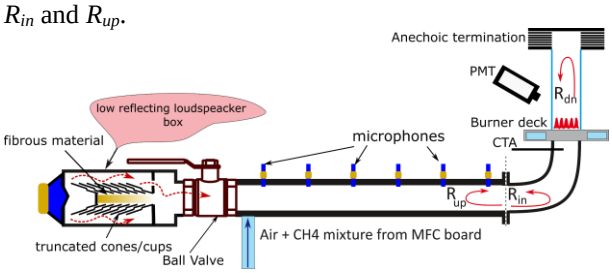

Fig. 1. Experimental setup for measuring the growth rate.

Test setup

Fully premixed multiple conical flames stabilized on the perforated burner deck installed on a water-cooled burner holder are tested. Two Mass Flow Controllers (MFC) are used to supply the air and methane to obtain the desired equivalence ratio and the mean velocity. The brass disk burner deck has 1 mm thickness with a hexagonal pattern of holes with a diameter of 2 mm and pitches of 4.5 mm (D2P4.5). The total area of the holes is 399 mm^2. The inner diameter of the gas path is 50 mm. The setup has been explained in more detail in [12].

As mentioned before, measuring the growth rate is a challenging task. It is needed to switch the situation of the system from stable to unstable condition and measure the acoustic pressure increment in the time domain. The switching time should be much shorter than the transient time to avoid affecting the growth rate measurement. To do so, the setup which is used in [12], has been modified. The upstream side has a broadband damper with |RC| less than 0.2 for the frequency range of 100-800 Hz. A ball valve is placed between the damper and the inlet of the gas mixture. By closing the ball valve, the upstream B.C. would be closed-end i.e. |Rup|~1, while when the valve is opened, the damper plays a role and the upstream B.C. would be semi-anechoic termination, i.e. $|R_{up}| < 0.2$ for frequencies higher than 100 Hz, as shown in Fig. 2. The closing time of the valve is less than (0.01 Sec) which is much shorter than the transient time for developing the limit cycle of instability of the system (0.3 sec). It is worth mentioning that by opening almost 10% of the valve, the semi-anechoic B.C. is obtained.

Besides, a constant temperature anemometer (CTA) and a photomultiplier tube (PMT) with OH filter are added to measure the FTF simultaneously for future studies. Two thermocouple type *K* and one type *S* have been used to measure the temperature at the burner deck and also at the burner downstream side.

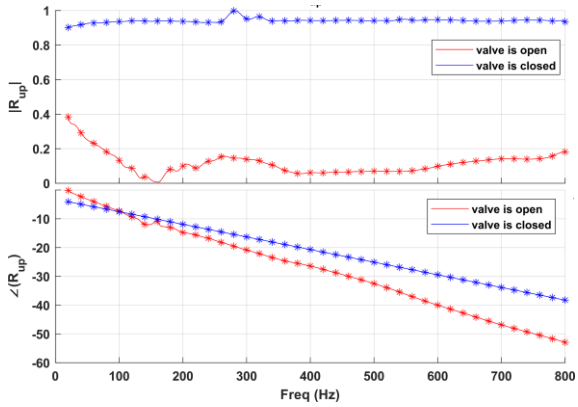

Fig. 2. Upstream RC while the ball valve is open or closed.

A loudspeaker is installed at the end part of the upstream side to provide a forced excitation supplied by the sequence of the pure tone signals. Software written in LabVIEW is implemented to control the amplitude of the excitation force, sampling rate, measuring time duration, as well as setting the desired range, steps of frequencies, and data preprocessing, etc.

The downstream part of the burner is a 110 mm long quartz tube with various terminations. These innovative terminations are capable to produce almost constant |RC| from 0.1 to 0.9 operating within the frequency range of

20-800Hz and installed at the downstream side of the flame/burner as plotted in Fig. 3.

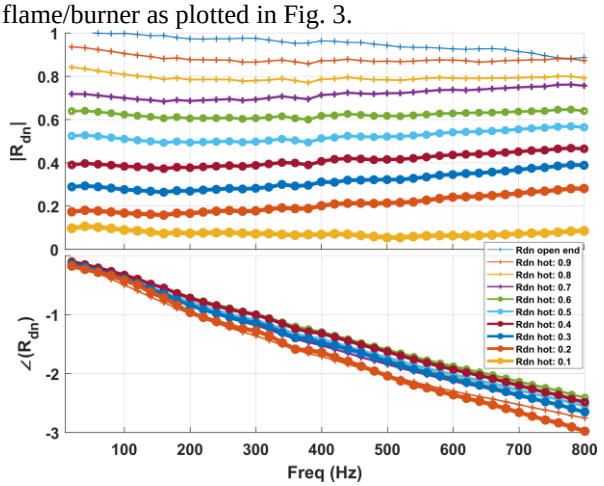

Fig. 3. Downstream RC of various innovated terminations.

R_{in} measurement

The impedance tube with 6 microphones including the low reflecting loudspeaker box (damper) at the upstream side, shown in Fig. 1, is used to measure the reflection coefficient R_{in} from the combination of a bended supply tube, the burner with flame, and the downstream subsystem. The damper enables the stabilization of the system for measuring R_{in} up to $|\mathrm{Rin}| < 5$ for the given conditions. By letting the system reach thermal stability, i.e. constant temperature at the burner deck and the downstream termination, the excitation signal with controlled amplitude is applied for 5 sec via the loudspeaker at discrete frequencies between 20 to 800 Hz with step of 10 Hz. The time domain data of 6 microphones, CTA, and PMT are recorded with sampling rate of 10000 sample/sec. The data from the microphones allow us to reconstruct the incident and reflected waves and next calculate the corresponding reflection coefficient following the conventional multi-microphones' method. The results are presented in Fig. 4 for the burner D2P4.5 at 65 cm/s mean velocity, equivalence ratio of 0.70, with ten various downstream terminations on the top of the 11 cm quartz tube.

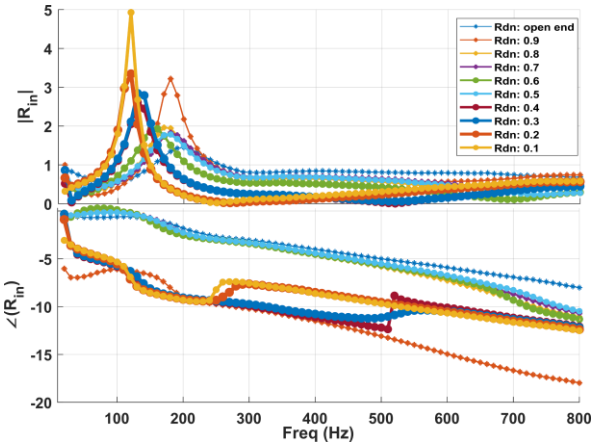

Fig. 4. Measured R_{in} for the burner D2P4.5 surface area 399 mm^2, mean velocity: 65 cm/s and $\varphi = 0.7$.

Method of measuring the growth/decay rate

For the growth/decay rate measurement, the loudspeaker is switched off. Next, within the data recording time of 10 sec, the ball valve is closed and opened several times to trigger the (in-)stability of the system on and off. The typical measured time signals of the closes to the burner microphone (No. 6-th), CTA, and PMT are illustrated in Fig. 5a.

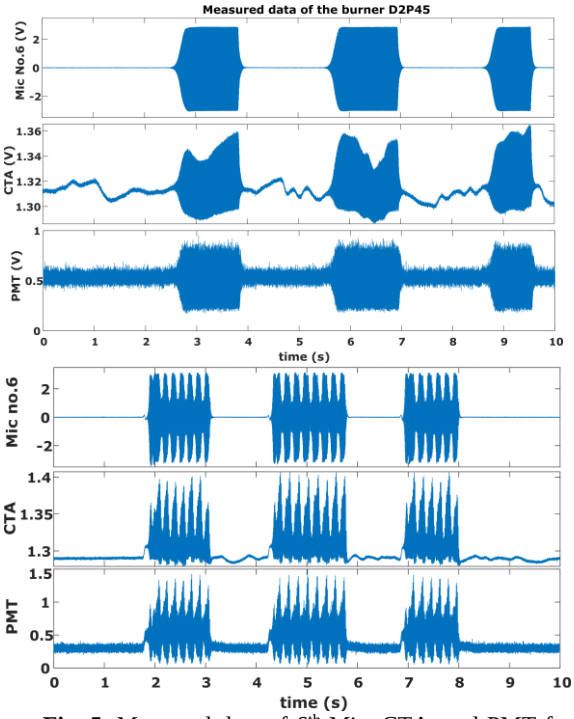

Fig. 5. Measured data of 6th Mic, CTA, and PMT for the burner D2P4.5 surface area 399 mm^2, mean velocity: 65 cm/s and $\varphi = 0.7$ with two different downstream B.C. (a) open-end (b) a termination with $|R_{dn}|$~0.4.

As shown in Fig. 5a, the valve is closed at ~2.51 sec which causes to switch the upstream B.C. to the closed-end. Accordingly, the stable operation of the system switches to an unstable one. The transition starts at the time instant of 2.51sec and ends at ~2.80 sec when a limit cycle establishes, and a tonal noise is heard. This test demonstrates the typical self-excitation sequence and the frequency of the tonal noise interpreted as the unstable frequency of the system. The rate of increasing acoustic pressure amplitude also provides the measure of growth rate which is explained in more detail in the next section. At 3.82 sec the valve is opened. Accordingly, the system transits back to stable operation and the signals provides a decay rate. In this example, the process of closing and opening the valve is repeated three times within 10 sec.

As the side result, Fig. 5b shows dynamics observed when the $|R_{dn}|$ is 0.4 or lower. In this case, the system does not have one dominant eigenfrequency. Hypothetically, a combination of the stable and unstable eigenfrequencies are interplaying. This phenomenon requires special investigation and is out of the scope of this paper. Therefore, the results which are shown later are for the downstream conditions with $|R_{dn}| > 0.4$.

Post-processing to determine the growth/decay rate

The Fast Fourier Transform (FFT) of the data at the developed limit cycle is calculated. The frequency at which the maximum of FFT occurs is considered as the unstable frequency. The instantaneous amplitude of the acoustic pressure signal is extracted with the Hilbert transform [17]. A low pass Butter filter is applied to the acoustic pressure signal to reduce the high frequency noise. Next, the logarithm of the amplitude of the pressure signal in the time domain is plotted, see Fig. 6. The turning point is located which is at the middle of the linear growth and decay regions. 50 points before and after of the turning point are selected to fit a linear polynomial curve to calculate the slope of the line. The number of points is increased from 50 to 1000 points to be sure that the slope converges to the unique number. Figure 7 shows the measured growth rate, slope, for three times of the opening and closing the ball valve for the case of the open-end downstream condition.

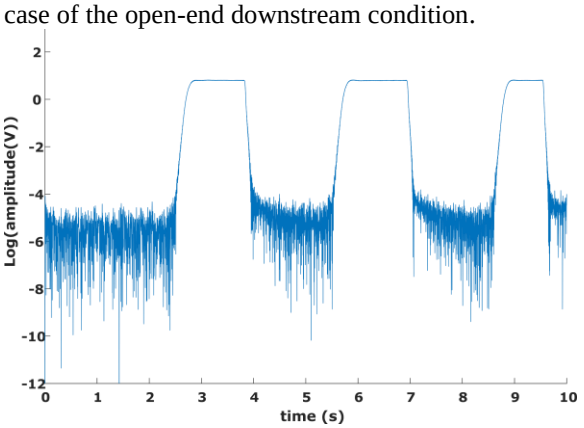

Fig. 6. A sample of the measured acoustic pressure signal.

As can be seen in Fig. 7, three lines converge to the almost same value signifying good repeatability of measuring the growth rate. The average of the final three points is considered as the growth/decay rate of the system at the given condition.

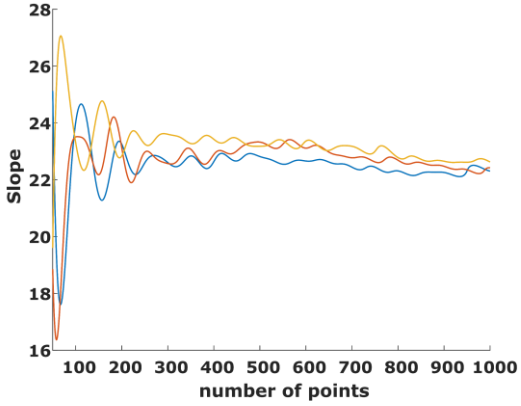

Fig. 7. Measured growth rate for the burner D2P4.5, surface area 399 mm^2, mean velocity: 65 cm/s, and $\varphi = 0.7$.

Calculating growth/decay rate from the first modeling strategy

The first modeling strategy is the direct method that we apply to establish the complex eigen frequencies of the system using the reflection coefficient form of the characteristic equation (Eq. (1)). The method involves estimating a rational function to fit the measured frequency responses of reflection coefficients $R_{up}(f)$ and $R_{in}(f)$ then establishing the location of the roots of Eq. (1). If the complex function $1- R_{up}(s)R_{in}(s)$ has zeros in the Right Half-Plane (RHP) of the complex domain, then the system is unstable and *vice versa* [12]. After checking the causality of the measured data with a special algorithm developed by Barannyk et al. [18], the spline interpolation command of MATLAB has been used to reduce the step size of the measured data to 1 Hz. Later, the discrete data of $1- R_{up}(f)R_{in}(f)$ are converted to the frequency response data-model. Next, by use of the transfer function estimation command in MATLAB a rational polynomial transfer function with a degree of 17 for the denominator is calculated. The fitting requires careful selection of the order of polynomials which is done manually. The degree is chosen such that the frequency response of the transfer function will be close to the measured data, no poles and zeros cancel each other, and by increasing the degree a new zero close to the origin does not appear. Then, zero and pole commands in MATLAB give the poles and zeros of the transfer function. The real part of zeros (σ) indicates the growth rate (if $\sigma>0$) or the decay rate (if $\sigma<0$) and the imaginary part would be the unstable eigenfrequency (if $\sigma>0$) or the stable eigenfrequency (if $\sigma<0$).

Calculating the growth rate from the second strategy

The second strategy is based on the polar plot of the measured $1-R_{in}(f)\ R_{up}(f)$ in the frequency domain. Using the well-known argument principle, the system stability can be determined by counting the number of turns of the graph around the origin. If the graph turns around the origin, then the system will be unstable otherwise it will be stable for the case that the function would be causal. For the polar plot, it is needed to either measure with a smaller step or use interpolation. In this work, the spline interpolation command of MATLAB has been used to reduce the step size to 1 Hz.

Kopitz and Polifke [13] showed that the unstable frequency is approximately equal to the frequency where the distance between the polar plot of OLTF and the critical point (-1) attains a local minimum. The growth rate is approximately equal to the minimum distance from the critical point to the OLTF image curve divided by the scaling factor of the mapping.

In the present work, instead of OLTF, we cut the loop into two parts, and measure each part separately, i.e. R_{in} & R_{up}, then put them together in the characteristic equation $1-R_{in}(f)\ R_{up}(f)$ which is a closed loop. Hence, the critical point would be the origin. The scale factor is then estimated as the length of the arc between one point before and after the derived point of unstable frequency divided by $2\Delta\omega$. For instance, in Fig. 8 the polar plot of $1-R_{in}(f)\ R_{up}(f)$ is depicted for the case of the burner D2P4.5 for the open-end downstream condition when the ball valve is closed. Figure 8 also shows the point where the minimum distance between the origin and points on the polar plot which are belongs to the left side relative to the origin has happened. The minimum distance is

0.2632 and the frequency of that point is 183 Hz that is considered as the unstable frequency. Next, the growth rate can be derived from the minimum distance divided by the length of arc between the points which correspond to 182 and 184 Hz divided by $(2 * 2\pi)$ which would be 20.1 sec^{-1}.

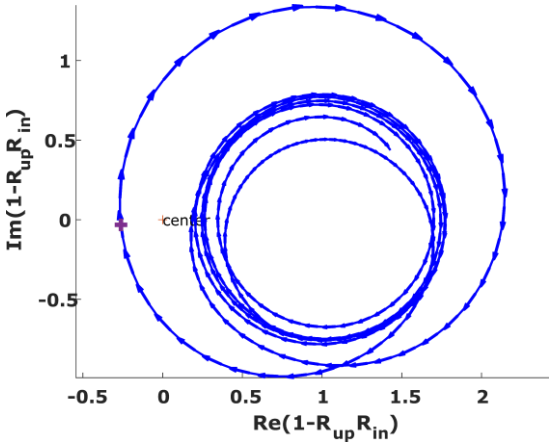

Fig. 8. Polar plot of $|1 - R_{up}(f)\, R_{in}(f)|$ with frequency step of 1 Hz for the burner D2P4.5 surface area 399 mm^2, v: 65 cm/s and $\varphi = 0.7$, R_{up} is as the closed end and R_{dn} is as the open end.

Results and discussion

All explained procedures have been performed for ten various downstream terminations when the ball valve is open, also for measuring the growth rate when the ball valve is closed. The results of measured and calculated unstable frequencies and the growth/decay rates are provided in Table. 1 for the six different acoustic downstream boundary conditions. As can be seen in Table. 1, the measured unstable frequencies match with the frequencies calculated by both methods with a discrepancy of less than 2 Hz. The correspondence between the measured growth rates and ones calculated from the first strategies is very good (deviations are less than 7 sec^{-1} in most cases), but for the second strategy, the deviation is up to 30 sec^{-1}. The unstable modes are highlighted with olive-green shading in the Table 1. The stable eigenfrequencies calculated from both strategies are matching well i.e. the stable frequencies have the accuracy of 2 Hz while for the decay rate of most cases, it is less than 11 sec^{-1} (shown with gray highlight).

Downstream Condition	Measured results		Calculated from 1st strategy (Complex domain)		Calculated from 2nd strategy (Frequency domain)	
	Unstable freq. (Hz)	Gr./De. rate (sec^{-1})	Eigen freq. (Hz)	Gr./De. rate (sec^{-1})	Eigen freq. (Hz)	Gr./De. rate (sec^{-1})
Open end	180.7	22.7±0.5	53.3±0.8	-79.2±12	53	-86.6
			114±27	-312±70	99	-363.0
			182.7±0.2	22.3±1	183	20.1
		-38.5±4	289.6	-27±2	290	-28.3
$\|R_{dn}\|$~0.9	175	77.1±1	32±2	-155±30	50	-547
			94.4±10	-150±50	82	-575.5
			178	74.1±0.5	177	39.9
		-48.1±4	273.7	-34.9±0.5	273	-38.9
$\|R_{dn}\|$~0.8	175.7	58.3±0.7	24±7	-177±50	-	-
			78.2±2.5	-150.3±20	77	-309
			177.2	49.7±0.6	178	35.4
		-68.5±6	281.5	-52.3±1.5	281	-63
$\|R_{dn}\|$~0.7	176.7	51±0.3	23.1	-285	-	-
			71.5±3	-168.7±30	70	-278
			179.3	45.1±0.5	179	33.7
		-59.4±4	283.6	-44.2±2	283	-48.7
$\|R_{dn}\|$~0.6	173.8	57.8±0.2	81.4±0.5	-86±8	82	-96.2
			169	33	169	27.3
		-91.8±3	281.9	-76.6±3	282	-112
$\|R_{dn}\|$~0.5	176.7	49.4±1	72.9±2	-125±9	71	-207
			174.1	43.1±1	174	32.8
		-47.5±7	283.1	-51.7±2	283	-61

Table 1. Results of comparing the Experimental data with two Theoretical strategies.

Conclusion

The experimental setup which allows studying thermoacoustic phenomenon in detail has been developed. The setup is unique due to the special equipment and the apparatuses that are added to the common impedance tube. One can measure the reflection coefficient of acoustical active elements, e.g. flame, with a magnitude of up to 10 because of the innovative compact damper which is added to the loudspeaker box. One CTA and one PMT are included in the impedance tube with six microphones to measure the FTF and R_{in} simultaneously. Nine compact size acoustic terminations, in a wide range between the anechoic end and the open-end, have been designed and made to produce various downstream acoustic boundary conditions. It is a promising technique to study the effect of the acoustic boundary conditions on the FTF experimentally. A ball valve has been added to the setup which can also switch

the upstream boundary condition from the closed end to semi-anechoic end such that one can measure the growth/decay rate of the instability. Moreover, it may provide more information in the transient regime to reconstruct the actual flame transfer function in the complex domain.

Furthermore, two theoretical approaches which provide the analysis of the thermoacoustic system in the complex and frequency domains are proposed. A new dispersion relation ($1- R_{up} R_{in}=0$) has been used in both approaches, which needs fewer measurements (only two acoustic measurements) and is more straightforward. Moreover, one does not need any specific *a-priori* information about the flame-acoustics interaction or acoustics properties of the (hot) downstream subsystem of the appliance.

The results of measurements and comparison of them with theoretical modeling reveal the following. First, by selecting a causal rational polynomial transfer function, it is possible to predict accurate eigenfrequencies of the system. Second, Kopitz and Polifke method could be used for $1-R_{up}(f)R_{in}(f)$ polar graph to predict eigenfrequencies with good accuracy, then there is no need to estimate the system transfer function.

Acknowledgments

The authors wish to thank the Netherlands Organization for Scientific Research (NWO) for the financial support under project number 16315 (STABLE).

References

[1] B. Schuermans, Modeling and control of thermoacoustic instabilities, Ph.D. Thesis, EPFL, Lausanne, 2003. https://doi.org/10.5075/epfl-thesis-2800.

[2] M. Manohar, Thermo-Acoustics of Bunsen Type Premixed Flames, 2011. https://doi.org/10.6100/IR695314.

[3] M. Zhu, A.P. Dowling, K.N.C. Bray, Flame transfer function calculations for com- bustion oscillations, in: Proc. ASME TURBO EXPO, New Orleans, 2001.

[4] N. Noiray, D. Durox, T. Schuller, S. Candel, A unified framework for nonlinear combustion instability analysis based on the flame describing function, J. Fluid Mech. 615 (2008) 139–167. https://doi.org/10.1017/S0022112008003613.

[5] C.O. Paschereit, B. Schuermans, W. Polifke, O. Mattson, Measurement of transfer matrices and source terms of premixed flames, J. Eng. Gas Turbines Power. 124 (2002) 239–247. https://doi.org/10.1115/1.1383255.

[6] N.N. Ã, B. Schuermans, Theoretical and experimental investigations on damper performance for suppression of thermoacoustic oscillations, J. Sound Vib. 331 (2012) 2753–2763. https://doi.org/10.1016/j.jsv.2012.02.005.

[7] L. Magri, M.P. Juniper, Sensitivity analysis of a time-delayed thermo-acoustic system via an adjoint-based approach, J. Fluid Mech. 719 (2013) 183–202. https://doi.org/10.1017/jfm.2012.639.

[8] G. Rigas, N.P. Jamieson, L.K.B. Li, M.P. Juniper, Experimental sensitivity analysis and control of thermoacoustic systems, J. Fluid Mech. 787 (2015). https://doi.org/10.1017/jfm.2015.715.

[9] N. Noiray, A. Denisov, A method to identify thermoacoustic growth rates in combustion chambers from dynamic pressure time series, Proc. Combust. Inst. (2017). https://doi.org/10.1016/j.proci.2016.06.092.

[10] C.F. Silva, T. Runte, W. Polifke, L. Magri, Uncertainty quantification of growth rates of thermoacoustic instability by an adjoint helmholtz solver, J. Eng. Gas Turbines Power. 139 (2017). https://doi.org/10.1115/1.4034203.

[11] D. Zhao, Thermodynamics-Acoustics Coupling Studies on Self-Excited Combustion Oscillations Maximum Growth Rate, J. Therm. Sci. 29 (2020). https://doi.org/10.1007/s11630-020-1361-8.

[12] M. Kojourimanesh, V. Kornilov, I.L. Arteaga, P. de Goey, Thermo-acoustic flame instability criteria based on upstream reflection coefficients, Combust. Flame. 225 (2021) 435–443. https://doi.org/10.1016/j.combustflame.2020.11.020.

[13] J. Kopitz, W. Polifke, CFD-based application of the Nyquist criterion to thermo-acoustic instabilities, J. Comput. Phys. 227 (2008) 6754–6778. https://doi.org/10.1016/j.jcp.2008.03.022.

[14] P.G.M. Hoeijmakers, Flame-acoustic coupling in combustion instabilities, Ph.D. Thesis, Technical University of Eindhoven, 2014. https://doi.org/10.6100/IR762773.

[15] G. Lombardi, B. Neri, On the Relationships Between Input and Output Stability in Two-Ports, IEEE Trans. Circuits Syst. I Regul. Pap. 66 (2019) 2489–2495. https://doi.org/10.1109/TCSI.2019.2898479.

[16] F. Boudy, D. Durox, T. Schuller, G. Jomaas, Ś. Candel, Describing function analysis of limit cycles in a multiple flame combustor, J. Eng. Gas Turbines Power. 133 (2011) 1–8. https://doi.org/10.1115/1.4002275.

[17] M. Schumm, E. Berger, P.A. Monkewitz, Self-excited oscillations in the wake of two-dimensional bluff bodies and their control, J. Fluid Mech. 271 (1994) 17–53. https://doi.org/10.1017/S0022112094001679.

[18] L.L. Barannyk, H.A. Aboutaleb, A. Elshabini, Spectrally Accurate Causality Enforcement using SVD-based Fourier Continuations for High Speed Digital Interconnects, IEEE Trans. Components. 5 (2015) 991–1005. https://doi.org/10.1109/TCPMT.2015.2444388.